Advanced Composite Materials
Publication details, including instructions for authors and subscription information:
http://www.tandfonline.com/loi/tacm20

Interlaminar Fracture Toughness of 5 Harness Satin Woven Fabric Carbon Fiber/Epoxy Composites

Toshio Ogasawara [a], Akinori Yoshimura [a], Takashi Ishikawa [a], Ryuya Takahashi [b], Nobuyuki Sasakib [b] & Takeshi Ogawa [b]

[a] Aerospace Research and Development Directorate, Japan Aerospace Exploration Agency (JAXA), 6-13-1 Osawa, Mitaka-shi, Tokyo 181-0015, Japan

[b] College of Science and Engineering, Aoyama-Gakuin University, 5-10-1 Fuchinobe, Chuo-Ku, Sagamihara-shi, Kanagawa 252-5258, Japan

Version of record first published: 17 Jul 2012.

To cite this article: Toshio Ogasawara , Akinori Yoshimura , Takashi Ishikawa , Ryuya Takahashi , Nobuyuki Sasakib & Takeshi Ogawa (2012): Interlaminar Fracture Toughness of 5 Harness Satin Woven Fabric Carbon Fiber/Epoxy Composites, Advanced Composite Materials, 21:1, 45-56

To link to this article: http://dx.doi.org/10.1163/156855112X626219

VSP

Advanced Composite Materials 21 (2012) 45–56

ADVANCED COMPOSITE MATERIALS
brill.nl/acm

Interlaminar Fracture Toughness of 5 Harness Satin Woven Fabric Carbon Fiber/Epoxy Composites

Toshio Ogasawara [a,*], **Akinori Yoshimura** [a], **Takashi Ishikawa** [a], **Ryuya Takahashi** [b], **Nobuyuki Sasaki** [b] **and Takeshi Ogawa** [b]

[a] Aerospace Research and Development Directorate, Japan Aerospace Exploration Agency (JAXA), 6-13-1 Osawa, Mitaka-shi, Tokyo 181-0015, Japan

[b] College of Science and Engineering, Aoyama-Gakuin University, 5-10-1 Fuchinobe, Chuo-Ku, Sagamihara-shi, Kanagawa 252-5258, Japan

Received 22 June 2011; accepted 10 December 2011

Abstract

This paper presents experimentally obtained results of mode-I and mode-II interlaminar fracture toughness (G_{IC} and G_{IIC}) of unidirectional and 5 harness satin (5HS) woven fabric carbon fiber/epoxy composites (CFRPs). The mode-I delamination resistance of 5HS specimens, which was evaluated using a double cantilever beam (DCB) method, depends on the weave pattern and the ply stacking sequence at the delamination growth plane. Higher toughness was observed for crack propagation between surfaces with more transverse bundles (L–T and T–T plane) than those with more longitudinal bundles (L–L plane) because of transverse tow delamination pinning the crack and causing it to arrest. The intrinsic mode-I fracture toughness values of the 0°/0°, 0°/90° and 90°/90° fiber combinations were estimated from the G_{IC} values obtained from three kinds of 5HS specimens which have different mid-plane stacking patterns (L–L, L–T and T–T). The G_{IC} of 0°/0° combination corresponded to that of unidirectional specimen. The G_{IC} of 0°/90° combination was almost identical to that of 90°/90° combination. Results suggest that the interlaminar fracture toughness of woven fabric composites can be estimated from the G_{IC} of 0°/0° and 0°/90° (or 90°/90°) combinations.

Keywords

Textile composites, delamination, interlaminar fracture toughness, carbon fiber

1. Introduction

Woven fabric composite laminates possess higher damage resistance than unidirectional composite laminates, thereby providing more damage tolerance against delamination. The delamination behavior of woven fabric composites has been investigated in detail during the last two decades [1–10]. Weave patterns are generally

* To whom correspondence should be addressed. E-mail: ogasat@chofu.jaxa.jp
Edited by the JSCM

 DOI:10.1163/156855112X626219

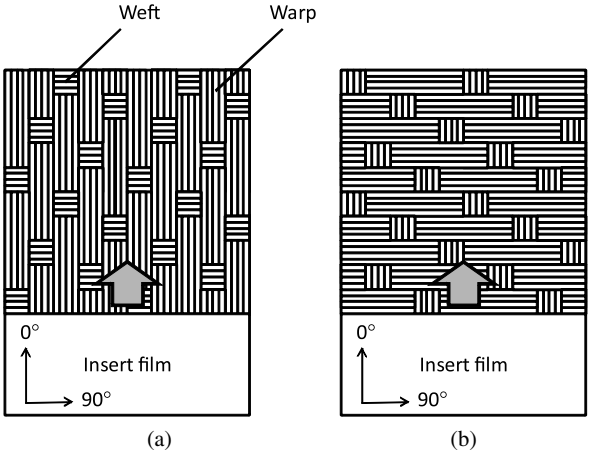

Figure 1. Schematic drawing of interlaminar crack growth in five harness satin woven composites. (a) L direction. (b) T direction. This figure is published in color in the online version.

represented using weave index n_g, i.e., $n_g = 2$ for plain weave, $n_g = 3$ for twill weave and $n_g \geqslant 4$ for satin weave fabrics [11]. Alif *et al.* reported that the crack resistance curves (R curves) of plain woven glass fiber/epoxy composites were almost flat, while those for twill and satin weave increased with crack growth [3]. Suppakul and Bandyopadhyay investigated the effects of the weave pattern on the mode-I interlaminar fracture toughness of glass/vinyl-ester composites. Their results show that the interlaminar fracture toughness increased with the weave index n_g, i.e., plain weave < (twill weave) < 4 harness satin (HS) < 8HS [5].

In addition to this, the interlaminar fracture toughness of twill and satin woven composites depends on the stacking sequence. Twill and satin weaves have ply asymmetry with one side predominantly warp and the other predominately weft. Schematic drawings showing 5-harness satin (5HS) woven fabrics are presented in Fig. 1. In this paper, warp (L) and weft (T) designates the fabric side that is predominately warp (longitudinal) and weft (transverse) bundles along the delamination growth, respectively. The delamination resistance of twill and harness satin weaves depends on the ply stacking at the delamination growth plane. There are three combinations, namely, L–L, L–T and T–T, as presented in Fig. 2. Alif *et al.* [4], Kotaki and Hamada [9] and Gill *et al.* [10] reported that higher toughness was observed for crack propagation between surfaces with more transverse bundles (T–T and L–T plane) than those with more longitudinal bundles (L–L plane). This was attributed to transverse fibers pinning the crack and causing it to arrest. Alif *et al.* observed debonding of transversely oriented yarns at the crack plane and crack branching around the debonded yarn in fracture surfaces of 5HS woven carbon/epoxy composites after DCB tests.

Studies reported previously in the literature showed that the interlaminar fracture toughness is influenced strongly by the weave surface texture derived from the weave pattern and the stacking sequence. However, there has been little quantitative

discussion of the effects of the weave surface texture on delamination resistance. Herein, we assess the influence of weave pattern and stacking sequence on the mode-I and mode-II interlaminar fracture toughness of unidirectional and 5HS woven fabric carbon fiber/epoxy composite laminates. Furthermore, based on experimentally obtained results, a simple method to estimate the fracture toughness of woven fabric composite laminates is proposed.

2. Experimental

2.1. Materials

The materials used for this study are unidirectional and 5HS woven carbon fiber/epoxy composites (T800H-12K/3633; Toray Co. Ltd, Japan). Typical mechanical properties are presented in Table 1 [12]. The number of fibers in a tow was 12 000. The tow width of 5HS weave fabric was approximately 1.5 mm. Three kinds of 5HS woven laminates were prepared, namely, L–L (warp–warp), L–T (warp–weft) and T–T (weft–weft) at the mid-plane satin face tow orientations, as shown in Fig. 2 and Table 2. A 0.025-mm-thick Kapton film was inserted at the mid-plane of

Table 1.
Mechanical properties of carbon fiber/epoxy composites (T800H/3633) [12]

	T800H/3633 (UD)	T800H/3633 (5HS)
E_L (GPa)	156	74.3
v_{LT}	0.34	0.05
E_T (GPa)	8.9	—
V_{TL}	0.02	—
G_{LT} (GPa)	4.7	4.8
V_f (%)	57	51

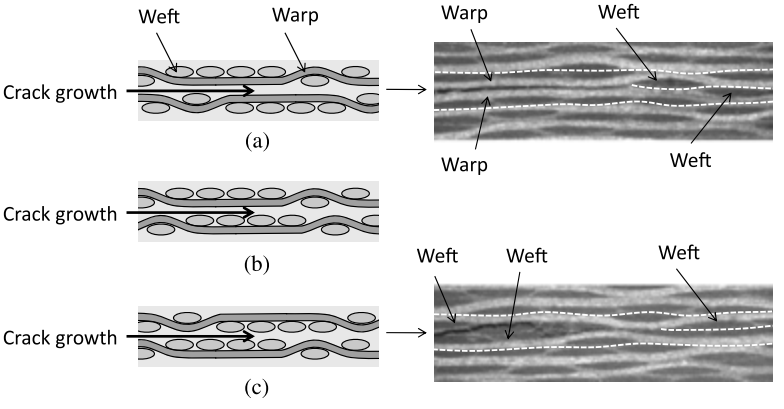

Figure 2. Schematic drawing and photographs of interlaminar crack propagation in 5 harness satin woven composites. (a) 5HS-L–L. (b) 5HS-L–T. (c) 5HS-T–T.

Table 2.
Mid-plane surface textures of DCB and ENF specimens

	Mid-plane	No. of plies	No. of samples	B (mm)	$2H$ (mm)	Crack starter
UD–0°	0°–0°	10	12	20	3	Film
5HS-L–L	L–L	14 ([7]s)	6	20	4.6	Film
5HS-T–T	T–T	14 ([7]s)	6	20	4.6	Film
5HS-L–T	L–T	16	8	12.5	5.2	Notch

* Insert-film or machined-notch length 40 mm.
** Initial crack length (a_0) 41–44 mm.

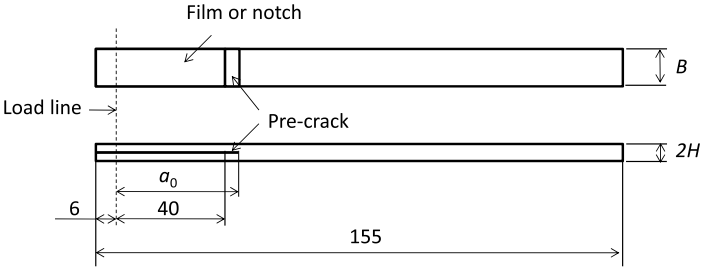

Figure 3. Schematic drawing of DCB test specimen. A pre-inserted Kapton film was used as the crack starter of UD, and 5HS-L–L and 5HS-T–T specimens. A machined notch (notch width 0.05 mm) was used for the crack starter for 5HS-L–T specimens. Before DCB testing, a precrack was induced using a flat-blade screwdriver.

unidirectional, 5HS-L–L and 5HS-T–T specimens for a starter crack. A machined notch was used for a starter crack of 5HS-L–T specimens. The notch width was 0.05 mm at the tip.

2.2. Double Cantilever Beam (DCB) Tests

Mode-I interlaminar fracture toughness was evaluated using a double cantilever beam method (DCB) in accordance with ASTM standard D5528 [13]. Figure 3 presents a schematic drawing of a DCB test specimen. Specimen width (B) and overall length (l) are, respectively, 20 and 155 mm. The thickness ($2H$) is approximately 3 mm for UD composite, 4.6 mm for 5HS-L–L and 5HS-T–T and 5.2 mm for 5HS-L–T specimens. The distance between the crack starter tip (film or machined notch) and the center of the aluminum end blocks was 40 mm. A precrack was induced by inserting a flat-blade screwdriver into the crack starter. It was difficult to introduce a straight precrack in the case of a machined notch (5HS-L–T), therefore only the specimens of which the precrack propagated to the middle interlayer (L–T plane) were used for the experiment. The precrack length was 1–4 mm, resulting in 41–44 mm of the initial crack length (a_0). Both edges of the specimen were coated with a thin layer of water-based white fluid to aid in visual detection

of delamination. The specimen was loaded under a constant displacement rate of 0.5 mm/min on an electrically driven test rig (4502; Instron Corp., USA). The loading rate was increased to 5 mm/min after the first 5 mm of delamination growth. The crack opening displacement (COD), load and crack length were measured at every 10 ± 2 mm of crack propagation. Data reduction was made using the modified beam theory method according to Japanese industrial standard (JIS K7086) [14] which is almost compatible with the ASTM D5528 [13]. The relation between compliance (C) and crack length (a) is expressed as shown below.

$$\frac{a}{2H} = \alpha_0 + \alpha_1 (BC)^{1/3}. \tag{1}$$

Therein, α_0 and α_1 are constants. In this study, no residual displacement was observed after the final unloading in all the specimens. Therefore, the compliance (C) was calculated using the load (P) and crack opening displacement (δ) as a gradient from the origin, i.e., $C = \delta/P$. Then G_{IC} is calculated as follows:

$$G_{IC} = \frac{3}{2(2H)} \left(\frac{P}{B}\right)^2 \frac{(BC)^{2/3}}{\alpha_1}. \tag{2}$$

2.3. End Notch Flexure (ENF) Tests

Mode-II tests were performed for UD, 5HS-L–L and 5HS-T–T specimens using a three-point bend, an end notched flexure (ENF) method performed according to JIS K7086 [14]. A schematic drawing is portrayed in Fig. 4. The specimens were positioned in the three-point bend fixture with a total span ($2L$) of 100 mm. The specimen width (B) and length (l) were 12.7 and 140 mm, respectively. An initial crack length (a_0) of 21–24 mm was achieved. The load was introduced to the specimen under a constant displacement rate of 0.5 mm/min until the crack propagated using an electrically driven test rig (4502; Instron Corp., USA). Mode-II fracture

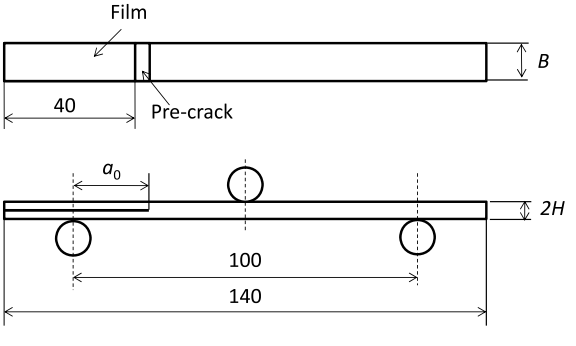

Figure 4. Schematic drawing of an end notch flexure (ENF) test configuration. A pre-inserted Kapton film was used for the crack starter.

toughness was calculated from the initial crack length (a_0), the ultimate load (P) and COD (δ) as follows [14]:

$$G_{\mathrm{IIC}} = \frac{9P^2Ca_0^2}{2B(2L^3 + 3a_0^3)} = \frac{9Pa_0^2\delta}{2B(2L^3 + 3a_0^3)}. \tag{3}$$

3. Experimental Results and Discussion

Typical load–displacement curves of UD, 5HS-L–L, 5HS-L–T and 5HS-T–T, which are obtained from DCB tests, are depicted in Fig. 5. The crack growth behavior of unidirectional specimens is stable, whereas the 5HS woven composite specimens exhibited similar saw-toothed load–displacement behaviors. Fracture toughness of the 5HS specimens was calculated from the points on the rising portion of the load–displacement curves associated with crack growth. Unstable crack growth behaviors in woven fabric composites have been reported in the literature [1–9].

The respective relations between the crack propagation length and fracture toughness G_{IC}, the so-called R curve, are depicted in Fig. 6(a)–(d) for UD, 5HS-L–L, 5HS-L–T and 5HS-T–T. The G_{IC} at $a_0 = 0$ corresponds to the initial fracture toughness, which is designated as G_{IC} in JIS K7086 standard. The load P for calculating the G_{IC} value was determined from the point of intersection between the load–displacement curve and the 5% offset line of the initial slope. The average G_{IC} values between 10 and 60 mm of crack propagation, which is designated as G_{IR} in JIS K7086, are presented in Table 3. The G_{IC} of the UD composite was much lower than those of 5HS composites, and the data show the least scattering. The G_{IC} values of 5HS composites exhibit considerable scattering. They are affected strongly by ply stacking at the delamination growth plane. The average G_{IR} of 5HS composites in ascending order was 5HS-L–L, 5HS-L–T, 5HS-T–T, which agrees with data from the literature [4, 9, 10]. The difference between 5HS-L–T and 5HS-T–T was not significant. The 5HS-L–L specimens showed a rising R-

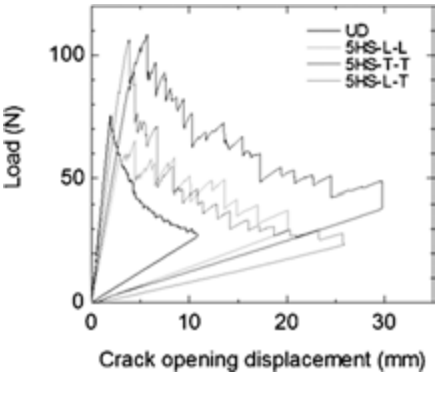

Figure 5. Typical load–displacement curves of unidirectional (UD), 5HS-L–L, 5HS-L–T and 5HS-T–T specimens. This figure is published in color in the online version.

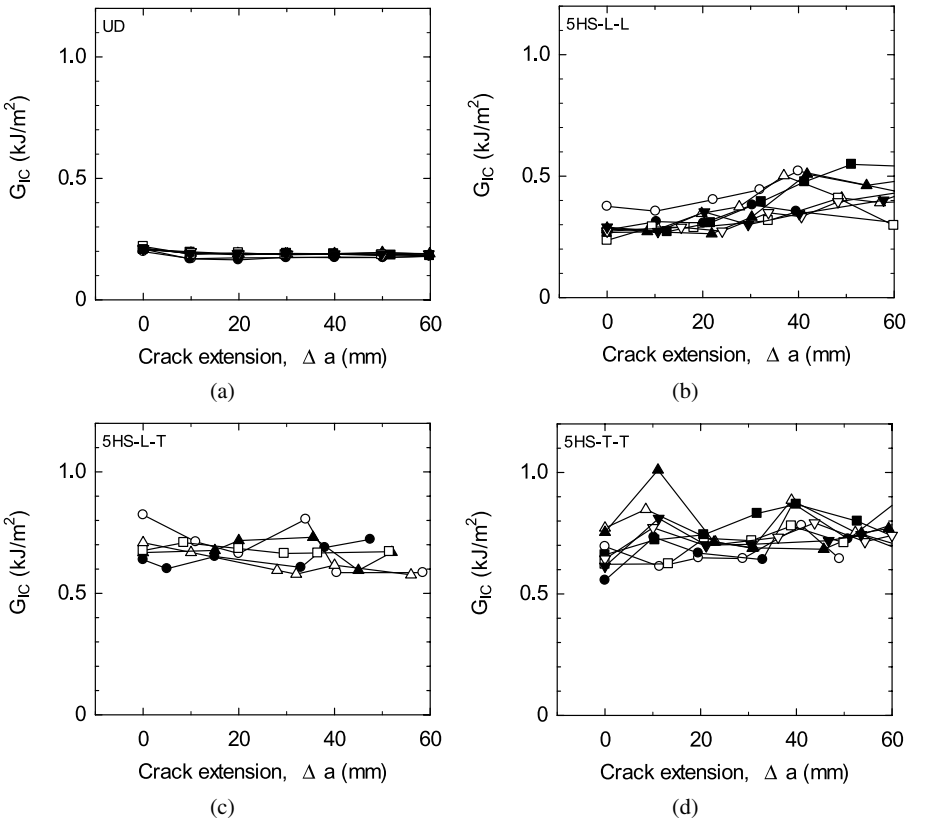

Figure 6. Crack resistance curves (R curves) of unidirectional (UD), 5HS-L–L, 5HS-T–T and 5HS-L–T specimens. (a) Unidirectional composites, $G_{IR} = 0.19$ (kJ/m^2), (b) 5 harness satin (L–L plane), $G_{IR} = 0.39$ (kJ/m^2), (c) 5 harness satin (L–T plane), $G_{IR} = 0.65$ (kJ/m^2), (d) 5 harness satin (T–T plane), $G_{IR} = 0.73$ (kJ/m^2).

Table 3.
Mode-I and mode-II interlaminar fracture toughness values (G_{IR} and G_{IIC}), and the areal ratio of each fiber bundle combination (0°/0°, 0°/90° and 90°/90°)

Fabrics and pattern stacking	Fracture toughness		A real ratio of each fiber bundle combination		
	G_{IR} (kJ/m^2)*	G_{IIC} (kJ/m^2)	0°/0°	0°/90°	90°/90°
UD-0	0.19	1.65	1	0	0
5HS-L–L	0.39	2.67	16/25	8/25	1/25
5HS-L–T	0.65	—	3/25**	19/25**	3/25**
5HS-T–T	0.73	2.56	1/25	8/25	16/25

* Average G_{IR} values between 10 and 60 mm of crack propagation.
** Probabilistic expectation based on statistical consideration.

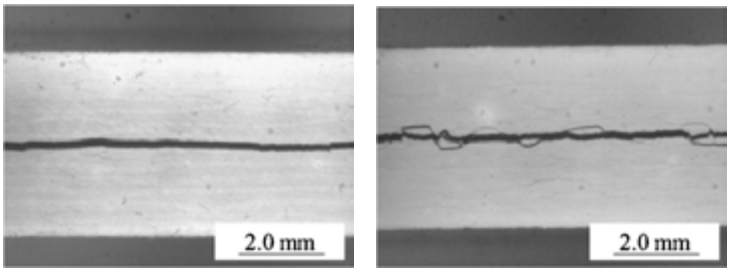

(a) (b)

Figure 7. Optical micrographs showing crack growth in 5HS (L–L) and 5HS (T–T) specimens. (a) 5HS-L–L specimen, (b) 5HS-T–T specimen.

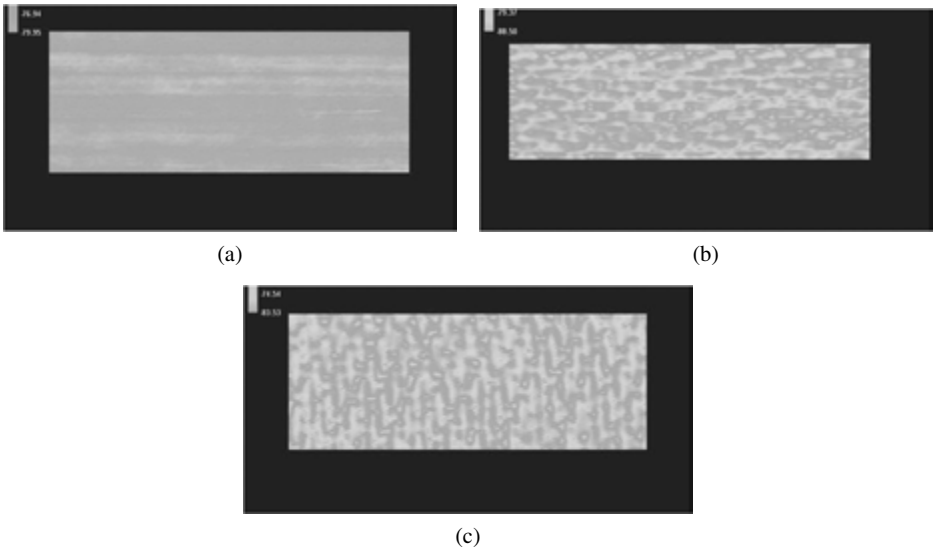

(a) (b)

(c)

Figure 8. Surface textures of delamination growth surfaces in UD, 5HS-L–L and 5HS-T–T specimens measured using a laser displacement sensor. (a) Unidirectional specimen (R_{max} 24 μm), (b) 5HS-L–L specimen (R_{max} 73 μm), (c) 5HS-T–T specimen (R_{max} 72 μm). This figure is published in color in the online version.

curve behavior, whereas the fracture toughness is almost independent of the crack propagation length in 5HS-L–T and 5HS-T–T specimens (flat R curves).

Optical photographs of 5HS-L–L and 5HS-T–T specimens illustrating the crack growth along interlaminar are presented in Fig. 7(a) and (b). Crack bowing, deflection, and branching, which are caused by the transverse fiber bundles, are visible in 5HS-T–T specimens. The surface textures of the delamination growth surfaces in UD, 5HS-L–L and 5HS-T–T specimens are depicted in Fig. 8(a)–(c). The data were obtained using a scanning a laser displacement sensor. Undulating patterns along the delamination growth direction are visible in the 5HS-T–T specimen. The observations demonstrate that the transverse fiber bundles contribute to the crack growth resistance, resulting in high interlaminar fracture toughness [3, 4].

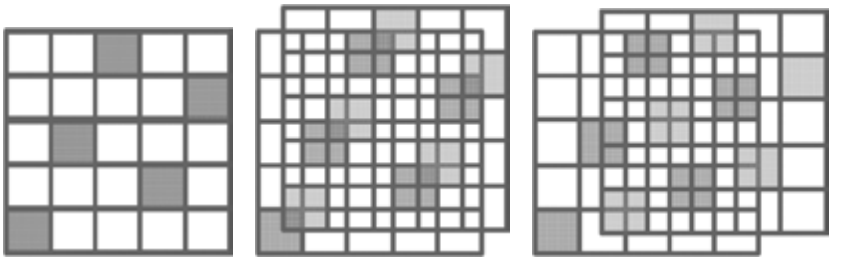

Figure 9. Schematic drawing showing microscopic fiber bundle combinations, 0°/0°, 0°/90° and 90°/90° at the delamination growth plane in a 5HS-L–T specimen. Red and blue squares respectively correspond to the 0° fiber bundles on the upper T surface and 90° bundles on the lower L surface. (a) Perfect overlapping of red and blue squares. The minimum areal ratio of 0°/0° and 90°/90° is zero, (b) partial overlapping of red and blue squares, (c) no overlapping of red and blue squares. The maximum areal ratio of 0°/0° and 90°/90° is 5/25 each. This figure is published in color in the online version.

Three kinds of fiber bundle combinations exist at the inter-layer of a 5HS woven composite, i.e., 0°/0°, 0°/90° and 90°/90° in Figs 1 and 9. Considering the geometric features of 5HS fabric, the areal ratios of each fiber bundle combination (0°/0°, 0°/90° and 90°/90°) in 5HS-L–L and 5HS-T–T specimens are easily determined, as shown in Table 3. However, the areal ratio in the 5HS-L–T specimen cannot be obtained deterministically. Schematic drawings illustrating the typical stacking pattern in a 5HS-L–T specimen are presented in Fig. 9. Red and blue squares correspond respectively to 0° bundles in the lower T surface and 90° bundles in the upper L surface. The minimum areal ratio of fiber bundle combination 0°/0° and 90°/90° is zero (Fig. 9(a)), and the maximum values are 5/25 each (Fig. 8(c)). The probability at the overlapping of blue and red squares is 20/25 (Fig. 8(b)). In this case, the expected values of areal ratios of fiber bundle combinations (0°/0°, 0°/0°, 90°/90°) in 5HS-L–T specimens are calculated as 3/25 ($= 3/4 \times 5/25 \times 20/25$), 19/25 and 3/25.

The fracture toughness (G_{IR}) of 5HS woven composites can be approximated by the sum of fracture toughness values of 0°/0°, 0°/90° and 90°/90° fiber bundle combinations as

$$G_{\mathrm{IR}} = a_1 G_{\mathrm{IR(0\text{-}0)}} + a_2 G_{\mathrm{IR(0\text{-}90)}} + a_3 G_{\mathrm{IR(90\text{-}90)}}, \tag{4}$$

where a_i is the areal ratio of each microscopic fiber bundle combination (0°/0°, 0°/0°, 90°/90°) and $G_{\mathrm{IR(0\text{-}0)}}$, $G_{\mathrm{IR(0\text{-}90)}}$ and $G_{\mathrm{IR(90\text{-}90)}}$ are the fracture toughness values of each combination. For 5HS fabric, the following equation is obtainable using a_i shown in Table 3.

$$\begin{pmatrix} 0.64 & 0.32 & 0.04 \\ 0.12 & 0.76 & 0.12 \\ 0.04 & 0.32 & 0.64 \end{pmatrix} \begin{pmatrix} G_{\mathrm{IR(0\text{-}0)}} \\ G_{\mathrm{IR(0\text{-}90)}} \\ G_{\mathrm{IR(90\text{-}90)}} \end{pmatrix} = \begin{pmatrix} G_{\mathrm{IR(5HS\text{-}L\text{-}L)}} \\ G_{\mathrm{IR(5HS\text{-}L\text{-}T)}} \\ G_{\mathrm{IR(5HS\text{-}T\text{-}T)}} \end{pmatrix}. \tag{5}$$

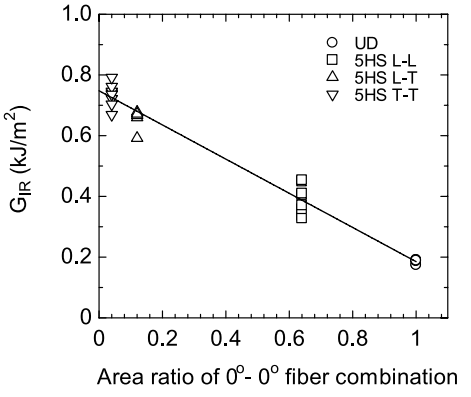

Figure 10. Mode-I interlaminar fracture toughness (G_{IR}) as a function of the area ratio of 0°/0° fiber bundle combination at the crack growth plane.

Therein, $G_{IR(5HS\text{-}L\text{-}L)}$, $G_{IR(5HS\text{-}L\text{-}T)}$ and $G_{IR(5HS\text{-}T\text{-}T)}$ respectively denote the fracture toughness of 5HS-L–L, L–T and T–T specimens. The right-hand side values are obtained from the experiments in this study. Therefore, the fracture toughness can be estimated for each fiber bundle combination (0°/0°, 0°/0°, 90°/90°).

The estimated values of $G_{IR(0\text{-}0)}$, $G_{IR(0\text{-}90)}$ and $G_{IR(90\text{-}90)}$ from the G_{IR} value of each 5HS composite listed in Table 3 are 0.21, 0.70 and 0.78 kJ/m^2, respectively. It is interesting that $G_{IR(0\text{-}0)}$ estimated here is almost identical to G_{IC} obtained from the unidirectional composites (0.19 kJ/m^2). This result implies that the basic approach used in this study is reasonable. Furthermore, $G_{IR(0\text{-}90)}$ is almost equal to $G_{IR(90\text{-}90)}$. The experimentally obtained results suggest that interlaminar fracture toughness is affected a great deal by 90° (transverse) fiber bundles.

The relation between the areal ratio of 0°/0° fiber bundle combination in a 5HS woven composite and the average fracture toughness (G_{IR}) between 10 and 60 mm of crack growth length is presented in Fig. 10. The results show good linearity. The result also implies that $G_{IR(0\text{-}90)}$ is equal to $G_{IR(90\text{-}90)}$. Using the relation described above, it is possible to predict the fracture toughness of a composite laminate which has other woven fabric pattern from $G_{IR(0\text{-}0)}$, $G_{IR(0\text{-}90)}$ (or $G_{IR(90\text{-}90)}$) and their corresponding areal ratios. For example, the areal ratio of 0°/0° combination in a plain woven fabric is 0.25 (0.5 × 0.5); therefore, G_{IR} is estimated as 0.61 kJ/m^2. The predicted values of twill and other harness satin woven composites are presented in Table 4. The G_{IC} increases with the weave index (n_g), which agrees with the experimentally obtained results reported by Suppakul and Bandyopadhyay [5].

The mode-II interlaminar fracture toughness (G_{IIC}) values, as obtained using ENF tests, are depicted in Table 3 in addition to G_{IC}. They are 1.65, 2.67 and 2.56 kJ/m^2, respectively, for UD, 5HS-L–L and 5HS-T–T specimens. The G_{IIC} values were naturally higher than the G_{IC} values, as expected, because of loading conditions under which fibers resist crack growth better because they are perpen-

Table 4.
Estimated values of mode-I interlaminar fracture toughness (G_{IR}) of plain, twill, and 8 harness satin (8HS) woven carbon fiber/epoxy composites (T800H/3633)

Fabrics and stacking pattern	Areal ratio of each fiber bundle combination			Estimated G_{IR} (kJ/m^2)
	0°/0°	0°/90°	90°/90°	
Plain weave	1/4	1/2	1/4	0.61
Twill-L–L	4/9	4/9	1/9	0.50
Twill-T–T	1/9	4/9	4/9	0.69
8HS-L–L	49/64	14/64	1/64	0.32
8HS-T–T	1/64	14/64	49/64	0.74

dicular to crack opening. The G_{IIC} values of 5HS-L–L specimens are identical to those of 5HS-T–T specimens. The effect of ply stacking pattern on G_{IIC} is not remarkable compared with G_{IC}. The ENF test provides only the initial value of mode-II interlaminar toughness. It suggests that the influence of fiber bridging is not significant. Therefore G_{IIC} might be independent of the ply stacking pattern.

4. Conclusions

The influence of the weave pattern and stacking sequence at the delamination growth plane on the mode-I and mode-II interlaminar fracture toughness of 5HS woven fabric carbon fiber/epoxy composite laminates was investigated.

1. Mode-I delamination resistance of 5HS specimens depends on the ply stacking sequence and weave pattern at the delamination growth planes. Higher toughness was observed for crack propagation between surfaces with more transverse bundles (L–T and T–T plane) than those with more longitudinal bundles (L–L plane). This was attributed to transverse fibers pinning the crack and causing it to arrest.

2. The intrinsic mode-I fracture toughness values of the 0°/0°, 0°/90° and 90°/90° fiber bundle combinations were estimated from G_{IR} values obtained from three kinds of 5HS composites which have different mid-plane stacking patterns. The G_{IR} of 0°/0° combination corresponded to that of unidirectional specimen, and the G_{IR} of 0°/90° combination was almost identical to that of 90°/90° combination. This fact suggests that the interlaminar fracture toughness of woven fabric composites can be estimated from the G_{IR} of 0°/0° and 0°/90° (or 90°/90°) combinations.

3. The mode-II interlaminar fracture toughness of 5HS woven specimens was almost independent of the stacking sequence at the delamination growth planes.

References

1. B. J. Briscoe, R. S. Court and D. R. Williams, The effect of fabric weave and surface texture on the interlaminar fracture toughness of aramid/epoxy laminates, *Compos. Sci. Technol.* **47**, 261–270 (1993).
2. I. Paris, P. J. Minguet and K. T. O'Brien, Comparison of delamination characterization for IM7/8552 composite woven and tape laminates, *ASTM STP* **1436**, 372–390 (2003).
3. N. Alif, L. A. Carlsson and J. W. Gillespie Jr., Mode I, mode II and mixed mode interlaminar fracture of woven fabric carbon/epoxy, *ASTM STP* **1242**, 82–106 (1997).
4. N. Alif, L. A. Carlsson and L. Boogh, The effect of weave pattern and crack propagation direction on mode I delamination resistance of woven glass and carbon composites, *Composites Part B* **29**, 603–611 (1998).
5. P. Suppakul and S. Bandyopadhyay, The effect of weave pattern on the mode-I interlaminar fracture energy of E-glass/vinyl ester composites, *Compos. Sci. Technol.* **62**, 709–717 (2002).
6. J.-K. Kim and M.-L. Sham, Impact and delamination failure of woven-fabric composites, *Compos. Sci. Technol.* **60**, 745–761 (2000).
7. Y. Wang and D. Zhao, Characterization of interlaminar fracture behaviour of woven fabric reinforced polymeric composites, *Composites* **26**, 115–124 (1995).
8. H. Hadavinia and H. Ghasemnejad, Effects of Mode-I and Mode-II interlaminar fracture toughness on the energy absorption of CFRP twill/weave composite box section, *Compos. Struct.* **89**, 303–314 (2009).
9. M. Kotaki and H. Hamada, Effect of interfacial properties and weave structure on mode I interlaminar fracture behaviour of glass satin woven fabric composites, *Composites Part A* **28A**, 257–266 (1997).
10. A. F. Gill, P. Robinson and S. Pinho, Effect of variation in fibre volume fraction on modes I and II delamination behavior of 5HS woven composites manufactured by RTM, *Compos. Sci. Technol.* **69**, 2368–2375 (2009).
11. T. Ishikawa and T.-W. Chou, Stiffness and strength behaviour of woven fabric composites, *J. Mater. Sci.* **17**, 3211–3220 (1982).
12. Composites Database System: JAXA-ACDB; Version 06-1, available at: http://www.jaxa-acdb.com/.
13. ASTM D5528, Standard test method for mode I interlaminar fracture toughness of unidirectional fiber-reinforced polymer matrix composites.
14. JIS K7086-1993, Testing methods for interlaminar fracture toughness of carbon fibre reinforced plastics, Japanese industrial standard (JIS) (English version is available).